INFECTION AND IMMUNITY, Feb. 2006, p. 821–829 Vol. 74, No. 2
0019-9567/06/$08.00+0 doi:10.1128/IAI.74.2.821–829.2006

Multifunctional Role of Choline Binding Protein G in Pneumococcal Pathogenesis

B. Mann,[1]† C. Orihuela,[1]† J. Antikainen,[2]† G. Gao,[1] J. Sublett,[1] T. K. Korhonen,[2] and E. Tuomanen[1]*

Department of Infectious Diseases, St. Jude Children's Research Hospital, Memphis, Tennessee 38105,[1] and General Microbiology, Faculty of Biosciences, University of Helsinki, Helsinki, FIN-00014, Finland[2]

Received 14 July 2005/Returned for modification 26 August 2005/Accepted 10 November 2005

Members of the choline binding protein (Cbp) family are noncovalently bound to phosphorylcholine residues on the surface of *Streptococcus pneumoniae*. It has been suggested that CbpG plays a role in adherence and increase virulence both at the mucosal surface and in the bloodstream, but the function of this protein has been unclear. A new sequence analysis indicated that CbpG is a possible member of the S1 family of multifunctional surface-associated serine proteases. Clinical isolates contained two alleles of *cbpG*, and one-third of the strains expressed a truncated protein lacking the C-terminal, cell wall-anchoring choline binding domain. CbpG on the surface of pneumococci (full length) or released into the supernatant (truncated) showed proteolytic activity for fibronectin and casein, as did CbpG expressed on lactobacilli or as a purified full-length or truncated recombinant protein. Recombinant CbpG (rCbpG)-coated beads adhered to eukaryotic cells, and TIGR4 mutants lacking CbpG or having a truncated CbpG protein showed decreased adherence in vitro and attenuation of disease in mouse challenge models of colonization, pneumonia, and bacteremia. Immunization with rCbpG was protective in an animal model of colonization and sepsis. We propose that CbpG is a multifunctional surface protein that in the cell-attached or secreted form cleaves host extracellular matrix and in the cell-attached form participates in bacterial adherence. This is the first example of distinct functions in virulence that are dependent on natural variation in expression of a choline binding domain.

Surface determinants are major contributors to pneumococcal virulence. The members of one family of 15 proteins share a repetitive choline binding domain that binds noncovalently to phosphorylcholine residues present on cell wall teichoic acid and membrane lipoteichoic acid (28). Each choline binding protein (Cbp) has a distinct function in the N terminus, while the C terminus harbors 2 to 10 choline binding repeats of a 20-amino-acid sequence (9, 26). Several Cbps have been implicated in virulence. These Cbps include LytA, which is required for daughter cell separation and lysis (24, 29); PspA, which decreases complement and lactoferrin deposition (27, 30); and CbpA, which is an adhesin for eukaryotic cells (25). CbpA and LytA are expressed predominantly when pneumococci are in the nasopharynx (25, 32), while PspA is expressed strongly in the bloodstream (20). A previous study suggested that CbpG is distinctive among Cbps in that it contributes to both mucosal and bloodstream virulence (11). Although a function for CbpG was not identified, a partial deletion mutant derived from insertion duplication mutagenesis (*cbpG*-$_{KKG}$) showed a 65% decrease in adherence to nasopharyngeal cells in vitro, a 75% decrease in the number of bacteria in the nasopharynges of mice at 48 h, and a >3-log increase in the 50% lethal dose for bacteremia in mice. These broad effects heightened interest in this protein as a vaccine candidate that could be useful for broad protection against colonization, as well as disease.

Recent reanalysis of the *cbpG* locus revealed 47% sequence similarity in amino acids 24 to 184 to the N terminus of the S1 family of multifunctional surface-associated serine proteases. Conservation of the catalytic triad consisting of H34, D87, and S159 was observed. Such bacterial proteinases have been found to have multiple functions; e.g., the C5a peptidase of group B streptococcus binds to fibronectin (2) and enhances invasion of epithelial cells (4), and the well-characterized Pla surface protease of *Yersinia pestis* is a plasminogen activator, an adhesin with affinity for laminin, and an invasin for human epithelium-like cells (reviewed in reference 16). By analogy, we considered the possibility that CbpG may also be multifunctional with distinguishable proteolytic and adhesive activities. This issue was not addressed by the mutant studied previously since 215 amino acids of the potentially proteolytic N terminus were not deleted (11). In this study, the function of CbpG was determined, and its role in infection of various body sites was reexamined by using murine models.

MATERIALS AND METHODS

Bacterial strains and growth conditions. Bacterial strains and recombinant plasmids used in this study are listed in Table 1. *Streptococcus pneumoniae* was grown either on tryptic soy agar (Difco, Detroit, MI) supplemented with 3% defibrinated sheep blood or in defined semisynthetic casein liquid medium supplemented with 0.5% yeast extract (C+Y) (17). The antibiotics added as appropriate included erythromycin (1 μg/ml), chloramphenicol (5 μg/ml), and kanamycin (400 μg/ml) (Sigma, St. Louis, MO). *S. pneumoniae* cultures were inoculated from a frozen stock and were incubated without aeration at 37°C in the presence of 5% CO_2. For the proteolysis assays, pneumococci were grown in tryptic soy broth supplemented with 0.2% yeast extract with appropriate antibiotics until the optical density at 620 nm (OD_{620}) was 0.75 to 0.80. *Escherichia coli* strains were grown in Luria-Bertani (LB) medium (Difco) at 37°C in an orbital shaker. The antibiotics used for *E. coli* growth were erythromycin (500 μg/ml) and ampicillin (100 μg/ml). The *Lactobacillus casei* derivatives were cultivated overnight in static API broth (1) with erythromycin (5 μg/ml).

Clinical isolates were obtained from several sources. Twenty-two nasopharyngeal isolates and 24 meningeal isolates were obtained from the St. Jude Hospital microbiology laboratory. Nineteen otitis media isolates were generously provided

* Corresponding author. Mailing address: St. Jude Children's Research Hospital, 332 N. Lauderdale Rd., Memphis, TN 38105. Phone: (901) 495-3114. Fax: (901) 495-3099. E-mail: elaine.tuomanen@stjude.org.
† B.M., C.O., and J.A. contributed equally to this work.

TABLE 1. Bacterial strains and plasmids used in this study

Strain or plasmid	Description	Reference or source
S. pneumoniae strains		
TIGR4	Serotype 4 meningeal isolate	28
TIGR4X	Bioluminescent TIGR4 bearing Tn*4001 luxABCDE* Km^r	21
CbpG-X	Bioluminescent CbpG-derivative of TIGR4X	This study
CbpG-$_{KKG}$X	Bioluminescent TIGR4X derivative expressing CbpG amino acids 1 to 215	This study
TIGR4R	Unencapsulated derivative of TIGR4	12
CbpG-$_{KKG}$R	Derivative of TIGR4R expressing CbpG amino acids 1 to 215	11
CbpG-R	Derivative of TIGR4R deficient in entire CbpG expression	This study
CbpGHK-R	Derivative of TIGR4R deficient in SP0386 histidine kinase	This study
CbpF-R	Derivative of TIGR4R deficient in CbpF expression	11
E. coli strains		
XL-1 Blue	Host strain for construction of recombinant plasmids	Stratagene
Top10F′	Host strain for TA cloning of recombinant plasmids	Invitrogen
BL21 (DE3)	Expression host for recombinant protein purification	Invitrogen
L. casei ATCC 393	Host strain for *Lactobacillus* expression	19
Plasmids		
pCR2.1	TA cloning vector	Invitrogen
PET32A	Expression vector with a thioredoxin fusion tag	Novagen
pET43G24-184	pET43a vector expressing CbpG amino acids 24 to 184	This study
pCAGGS	Eukaryotic expression vector	A. Portner
pLPMSSA3	*Lactobacillus* expression vector	1
pLPMSSA4	*Lactobacillus* expression vector with BamHI cloning site	This study
pLPMSSA4 (CbpG)	pLPMSSA4 vector expressing CbpG amino acids 1 to 285	This study

by S. Pelton, Boston, MA. Twenty pneumonia isolates were kindly provided by D. Musher, Houston, TX.

Sequencing of the *cbpG* locus. Using the TIGR4 gene database, primers were synthesized to amplify and sequence regions of the *cbpG* locus (Table 2). PCRs were performed using Sigma HotStart *Taq* polymerase (Sigma) and the following parameters: 94°C for 3 min, followed by 30 cycles of 94°C for 1 min, 57°C for 1 min, and 72°C for 3 min and then 72°C for 10 min. Genomic DNA for amplification was obtained from the pellet from 1 ml of culture, which was suspended and boiled in 100 μl of Tris buffer (10 mM Tris-HCl, pH 8.5); 5 μl was subsequently used for the PCR. Following amplification, the PCR product was purified using a PCR purification kit (QIAGEN, Valencia, CA) and sent to the St. Jude Children's Research Hospital Hartwell Center for nucleotide sequencing. The sequences retrieved were compared to the TIGR4 genome using the BLASTN program available at the NCBI website (http://www.ncbi.nlm.nih.gov/BLAST).

Construction of *cbpG* mutants. Mutant strains *cbpG*-$_{KKG}$ and *cbpF*- and the unencapsulated form of TIGR4 (TIGR4R) were constructed previously (11). *cbpG*- was constructed by PCR-mediated recombination and mutagenesis. In

TABLE 2. Primer pairs used for amplification of gene fragments and specific probes

Primer	5′–3′ sequence	Nucleotide coordinates (TIGR)
CbpG locus sequencing		
BMG4r	CACAGTTATTCCTGTCAAATTTTTTTGAC	369087-369059
BMG5f	GGATGCAAGGGAATATGACTTGGC	368976-368999
BMG5r	CCATCCTTCAGAATCATCTGC	369708-369688
Gene replacement mutagenesis		
GUPF	CTAGCGTGATTGAAAAGC	368297-368315
GUPR	CTTCTAAGTCTTATTTCCGCTGAAGTCGAATACGG	368716-368733
GDNF	GTCGCTTTTGTAAATTTGGCAAATCGCACTAGCC	369630-369645
GDNR	CTGTTTGAGGGCAGTAC	370731-370747
ERMF	GGAAATAAGACTTAGAAGCAAAC	
ERmR	CAAATTTACAAAAGCGACTC	
GHKUPF	GAAGGGAGAGGATGAAC	365177-365193
GHKUPR	CTTCTAAGTCTTATTTCCGGAAGGAGGTGAGAGC	365918-365933
GHKDNF	GAGTCGCTTTTGTAAATTTGGCTGCGAAATATCAAGGAG	366773-366790
GHKDNR	GCTGCTTCTAGCTCCTC	367555-367571
Northern analysis		
CbpGNde1	CATATGGTTTTATCTAAGTATTATGG	368734-368756
CbpGEco210	CTTCCATCCTTCAAGAG	369348-369364
CbpGHKF	GCAGGGCAAGAAGTGG	366140-366155
CbpGHKR	CCATATCTTCAACCCGCTCCTTG	366784-366806
CbpFF	GCGACAAATACAGTATTTGC	369670-369689
CbpFR	CGCGAATCAAAGCCACCATCC	370121-370138
Plasmid		
BMG24Bgl	AGATCTGATGATTAAAGATAATGTGTTAATTACAGCGG	
BMG184Xho	CTCGAGTTAGTTAATTTGATTAGCTCCATC	
GecoF2	GCGCGCGCGAATTCATGGTTTTATCTAAGTATTATG	
GxhoR2	GCGCGCGCCTCGAGTTAAATCCACTCACCAGATGAAGC	

short, three independent DNA fragments were amplified by PCR (with primers listed in Table 2). A fragment corresponding to the 437 bp upstream of *cbpG* was amplified using primers GUPF and GUPR. A fragment corresponding to a 1-kb region downstream of *cbpG* was amplified using GDNF and GDNR. A fragment corresponding to the 1-kb erythromycin cassette was amplified with primers ERMF and ERMR. GUPR and GDNF included sequences that corresponded to the upstream and downstream regions of the erythromycin resistance cassette. Equimolar concentrations of the three PCR fragments were mixed and amplified by PCR with the GUPF and GDNR primers. The resulting fragment mimicked the *cbpG* locus with *cbpG* replaced with erythromycin. *cbpGHK*- was constructed by the same method, using GHKUPF and GHKUPR to amplify a 750-bp fragment upstream of GHK and using GHKDNF and GHKDNR to amplify a 690-bp fragment downstream of *cbpGHK*. Equimolar concentrations of these two fragments were mixed with the erythromycin cassette and amplified with GHKUPF and GHKDNR. One microgram of the PCR fragment was transformed into TIGR4R using conventional methods. Transformants were grown in the presence of erythromycin, and TIGR4R transformants were grown in the presence of both erythromycin and chloramphenicol to maintain the capsule deletion. Chromosomal integration of the gene replacement was confirmed by sequencing with primers designed for sequences in the *cbpG* and *cbpGHK* loci (Table 2). For wild-type and mutant strains, the presence of CbpG in whole-cell lysates (0.1% Triton X-100), on the intact bacterial surface, secreted into the supernatant fluid, or released from the surface by 5% choline (by soaking for 10 min) was documented by loading fractions onto a prepared polyvinylidene difluoride membrane and probing with antibody to CbpG.

Northern blot hybridization. Wild-type TIGR4R and CbpG-R were grown in C+Y without antibiotics, and 5 ml was harvested at OD_{620} of 0.2, 0.4, 0.6, and 0.8. Each pellet was resuspended in RNAProtect (QIAGEN) for 15 min, centrifuged, and stored at −80°C. The bacteria were then lysed with a bead beater (RNAProtect prevented enzymatic or detergent lysis), and RNA was extracted using a modified version of the QIAGEN RNAEasy protocol. Probes for *cbpG*, hisitidine kinase, and *cbpF* were amplified by PCR using primers CbpGNdeI and CbpGEco210, primers CbpGHKF and CbpGHKR, and primers CbpFF and CbpFR (Table 2) and labeled with [α-^{32}P]dCTP (Amersham) by using a random primer labeling kit (Roche). Radioactivity was determined using a 455SI Phosphorimager (Molecular Dynamics).

Proteolysis assays with pneumococcal strains. Choline binding proteins were eluted from the bacterial surface with choline as described previously (11). Briefly, washed bacteria were incubated with 2% choline (Sigma) in phosphate-buffered saline (PBS) for 20 min at room temperature. Eluates were dialyzed for two nights against 50 mM Tris-HCl (pH 8.0) at 4°C, and eluates (20 μl) were incubated with 2 μg of fibronectin for 4 h or with 4 μg of α-casein for 3 h at 37°C. Degradation of fibronectin was assayed by Western blotting using anti-fibronectin antiserum, and degradation of α-casein samples was assayed by 15% sodium dodecyl sulfate (SDS)–polyacrylamide gel electrophoresis (PAGE).

Expression of recombinant CbpG. DNA corresponding to amino acids 24 to 184 of CbpG was PCR amplified from TIGR4 genomic DNA using primers BMG24Bgl and BMG184Xho (Table 2). The amplified DNA was purified and subcloned into the TA cloning vector pCR2.1 (Invitrogen, Carlsbad, CA). Clones were screened by digestion with EcoRI and sent for nucleotide sequencing at the Hartwell Center. Clones containing the correct in-frame sequence were digested with EcoRI and XhoI, and the resulting 600-bp fragment was gel purified (QIAGEN). The purified insert was ligated into the prepared thioredoxin fusion vector pET32a (Novagen, Madison, WI) and transformed into *E. coli* expression host strain BL21(DE3) (Invitrogen). BL21 containing the recombinant plasmid was grown in LB medium with ampicillin (100 μg/ml) to an OD_{620} of 0.6, and the recombinant protein was induced with 0.07 mM isopropyl-β-D-thiogalactopyranoside (IPTG) overnight at 25°C. Following induction, the bacteria were centrifuged and lysed with a Bugbuster (Novagen) used according to the manufacturer's protocol. The soluble fraction was purified over Ni^{2+} resin (Sigma), and the purified protein was cleaved overnight at room temperature with thrombin (5 U/mg; Novagen). Recombinant CbpG (rCbpG) was subsequently purified by gel filtration. Antiserum was produced in rabbits by Covance Immunological Services (Covance Inc., Princeton, NJ). To test for proteolysis, 4 μg of recombinant CbpG (amino acids 24 to 184) or the purified pET32 vector control was incubated for 20 h at 37°C with 4 μg of casein (Sigma) in a buffer consisting of 150 mM NaCl, 1 mM $CaCl_2$, 1 mM $MgCl_2$, and 50 mM Tris-Cl (pH 7.4). The samples were loaded in nonreducing sample buffer and subjected to SDS-PAGE. The gels were stained with SimplyBlue Safestain (Invitrogen) and analyzed for casein digestion.

Expression of CbpG on the surface of *L. casei*. Standard recombinant DNA techniques were used for expression of CbpG on the surface of *L. casei*. CbpG was PCR amplified from chromosomal DNA of strain T4 and cloned in the pLPMSSA4 vector, which was derived from the pLPMSSA3 vector (1, 19) by insertion of a BamHI cloning site between the signal sequence of CbsA and the LPXTG cell wall-anchoring motif (Table 1). The plasmid was electroporated into *L. casei* as described previously (23). Expression of the peptide on the surface of *L. casei* was confirmed by dot blotting and by indirect immunofluorescence with anti-CbpG antibody. For the dot blot analysis, bacterial cells (OD_{620}, 1.0) were dotted onto a nitrocellulose membrane, blocked with 2% bovine serum albumin–PBS, and probed with anti-rCbpG antiserum. The indirect immunofluorescence analysis was performed as described previously (22) with anti-rCbpG antiserum and tetramethylrhodamine isothiocyanate-labeled swine anti-rabbit antibodies (Dako).

For the proteolysis assay with α-casein (Sigma), 50 μl of a bacterial suspension (OD_{620}, 2.0) in 50 mM Tris-HCl (pH 8.0)–10 mM $CaCl_2$ was incubated with 10 μg of α-casein at 37°C for 18 h. Casein degradation was analyzed by Western blotting of 15% (wt/vol) SDS–PAGE gels with anticasein antibody (Axell, Accurate Chemical and Scientific Corp.). Proteolysis assays with fibronectin (BD Biosciences) were performed by incubating 20 μl of a cell suspension with 2 μg of fibronectin, and degradation was analyzed by Western blotting of an SDS-PAGE gel with antifibronectin antiserum (produced in rabbits by National Public Health Institute, Finland).

Expression of recombinant CbpG in 293T eukaryotic cells and protease activity. Full-length recombinant CbpG was amplified by PCR using oligonucleotides GecoF2 and GxhoR2 (Table 2). The 883-bp fragment was digested along with eukaryotic expression vector pCAGGS (provided by A. Portner) with restriction enzymes EcoRI and XhoI. The digested products were purified and ligated using T4 DNA ligase (New England Biolabs). The ligation reaction mixture was transformed into Novablue competent cells (Novagen) and grown on LB medium plates with ampicillin. A clone that contained the correct in-frame sequence was chosen by digestion with EcoRI and XhoI and DNA sequencing. 293T cells (also provided by the lab of A. Portner, St. Jude Hospital) were grown to 95% confluence in a six-well plate with Optimem containing 5% fetal bovine serum. Cells were transfected with 4 μg pCAGGS/CbpG DNA using Lipofectamine 2000 (Invitrogen). At 48 h after transfection, cells were lysed with 0.1% Triton X-100 and assayed by Western blotting with anti-CbpG for protein expression. To test for proteolytic activity, equal amounts of either CbpG-293T cell lysate or 293T control lysate were loaded onto a 4 to 16% Blue Casein zymogram gel (Invitrogen). The gel was electrophoresed for 110 min at 125 V. After electrophoresis, the gel was renatured for 30 min and developed overnight at 37°C using Novex zymogram renaturing and developing buffers (Invitrogen) according to the manufacturer's protocol. Protease activity was indicated by a clear zone in the blue gel.

In vitro adhesion assay. The A549 lung epithelial (ATCC), Detroit nasopharyngeal epithelial (ATCC), and $RBCEC_6$ rat brain endothelial (3) (provided by J. R. Weber, Berlin, Germany) cell lines were maintained in culture media at 37°C in the presence of 5% CO_2. For adhesion assays, cells were grown to 100% confluence in Terasaki plates (Robbins Scientific, Sunnyvale, CA). Prior to infection, cells were activated for 2 h at 37°C with human tumor necrosis factor alpha (10 ng/ml; Endogen, Woburn, MA). Bacterial cultures were grown to an OD_{620} of 0.6 and labeled with fluorescein isothiocyanate (1 mg/ml in 50 mM carbonate buffer; Sigma). Each well was inoculated with 1×10^5 CFU and incubated for 30 min at 37°C. The plates were washed and fixed with 2.5% glutaraldehyde (Sigma). The adherent bacteria were visually counted with a TE300 fluorescent microscope (Nikon, Melville, NY).

To demonstrate direct adherence capability, adhesion of rCbpG24-184-coated latex beads to endothelial cells was assessed. $RBCEC_6$ cells were seeded to 80% confluence in a 24-well plate. The cells were activated for 2 h with human tumor necrosis factor alpha (10 ng/ml) and fixed with 4% paraformaldehyde. The plates were blocked overnight in 1% bovine serum albumin. Fluoresbrite YG carboxylate microspheres (Polysciences, Inc.) were covalently coupled with rCbpG24-184 or thioredoxin control proteins according to the manufacturer's protocol. The protein-coupled beads were incubated with the $RBCEC_6$ cells for 30 min and washed four times with PBS. Adherent microspheres were quantified with a fluorescence microscope.

Monitoring of bioluminescent pneumococcal infections. TIGR4 was transformed with genomic DNA obtained from the bioluminescent strain D39 Tn*4001 luxABCDE* Km^r Xen7 (8). Transformants were screened for bioluminescence using an IVIS camera, and the brightest colonies were selected and passaged in the absence of antibiotics to verify that bioluminescence was stable. TIGR4 Xen 35 (TIGR4X) was selected for use in future studies. Bioluminescent *cbpG*-deficient mutants *cbpG*-$_{KKG}$X and *cbpG*-X were constructed by insertional duplication mutagenesis of TIGR4X and confirmed by PCR and sequencing. Exponential cultures of TIGR4X, *cbpG*-$_{KKG}$X, and *cbpG*-X (OD_{620}, 0.5) containing 10^8 CFU/ml were centrifuged, and the bacteria were washed in sterile PBS (BioWhittaker, Walkersville, MD). Washed pneumococci were suspended

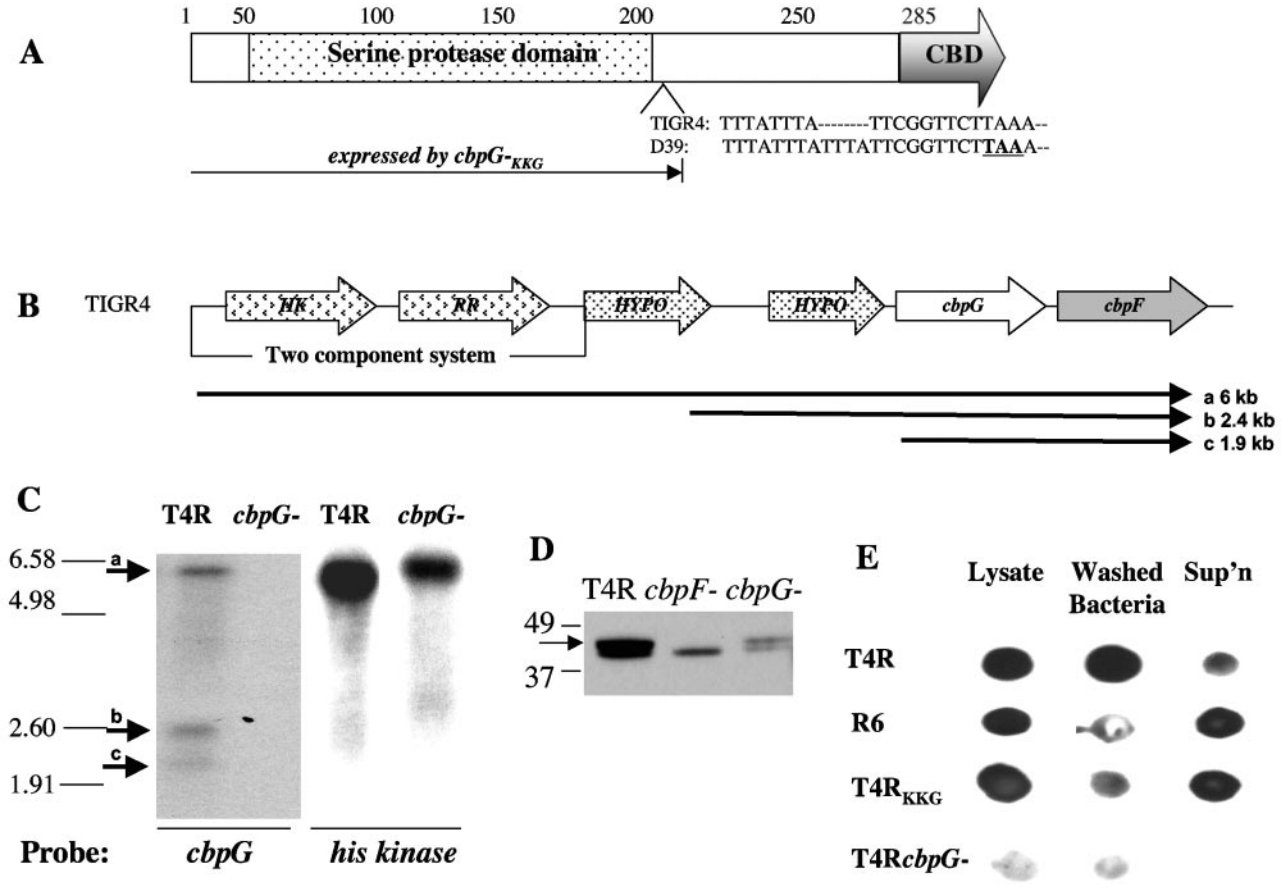

FIG. 1. Organization of the *cbpG* locus. (A) Regions of *cbpG* encoding a putative amino-terminal serine protease domain and the carboxy-terminal choline binding domain (CBD). Sequence analysis of D39 *cbpG* revealed insertion of TAAA that introduces a stop codon (boldface underlined TAA) at amino acid 203 that truncates the protein before the choline binding domain. An analogous truncation was created in mutant $cbpG_{-KKG}$, as indicated. (B) Schematic diagram of the *cbpG* locus annotated in the TIGR database. *HK*, histidine kinase; *RR*, response regulator; *HYPO*, hypothetical protein. Arrows a, b, and c indicate transcripts detected by the Northern analysis shown in panel C. (C) Northern blot analysis of *cbpG* and histidine kinase expression in TIGR4R (T4R) and the isogenic *cbpG-* mutant using the probes indicated at the bottom. Replacement of *cbpG* with the erythromycin cassette in the *cbpG-* mutant probed with the histidine kinase sequence increased the transcript size ~200 bp. The positions of size markers are indicated on the left. Arrows a, b, and c indicate transcripts shown in panel B. (D) Western blot analysis for expression of CbpF (arrow) in TIGR4 (T4R) and isogenic *cbpF-* and *cbpG-* mutants. The cross-reactive band present in all lanes is CbpC, as determined by mass spectrometric analysis. (E) Dot blot analysis using anti-CbpG antibody of washed whole-cell lysate, washed intact bacteria, and culture supernatant (Sup'n) for TIGR4, R6, and mutants.

in PBS at various concentrations that were confirmed by serial dilution and plating on blood agar plates.

Female BALB/cJ mice (Jackson Laboratory, Bar Harbor, ME) that were 4 to 5 weeks old were maintained in a biosafety level 2 facilities. All experiments were done with mice under general anesthesia with either inhaled isoflurane (2.5%; Baxter Healthcare Corp., Deerfield, IL) or intraperitoneal injection of MKX (1 ml ketamine [100 mg/ml; Fort Dodge Laboratories, Fort Dodge, IA)], 5 ml Xylazine [100 mg/ml; Miles Laboratories, Shawnee Mission, KS], and 21 ml PBS at a dose of 0.05 ml/10 g). Bacteria were introduced either by intranasal administration of 10^7 CFU in 25 μl PBS, by intratracheal administration of 10^6 CFU in 100 μl PBS, or by intravenous injection of 10^5 CFU in 100 μl PBS in the tail vein. Following challenge, subsets of 6 to 10 mice were randomly selected at 24-h intervals for each experimental group and imaged using the IVIS charge-coupled device camera. Following imaging, mice were lavaged intranasally and sacrificed for collection of pertinent organs and body fluids. The bacterial titers in nasopharyngeal lavages, blood, and cerebrospinal fluid (CSF) were determined by standard serial dilution and plating. Lungs were weighed and homogenized in 10 ml PBS (Tissue Tearor; Biospec Products Inc., Bartlesville, OK), and the number of bacteria per gram of lung tissue was determined. A statistical analysis was performed using a nonparametric independent group analysis (Mann-Whitney rank sum).

For protection studies, three groups of 4-week-old female BALB/c mice (10 to 12 mice per group) were immunized intramuscularly with 10 μg of either thioredoxin control protein or rCbpG on days 0, 14, and 28. Antibody titers in the blood were determined by an enzyme-linked immunosorbent assay, and at day 42 mice were infected intranasally with 10^7 wild-type TIGR4 cells and then monitored for mortality. At 24, 48, and 72 h postinfection, nasal passages were lavaged and blood was extracted from the tail, diluted, and plated on blood agar to test for colonization and bacteremia, respectively.

RESULTS

Alleles of the *cbpG* locus in clinical strains. Comparison of the sequence of *cbpG* of TIGR4 to the sequences of laboratory strains D39 and R6 revealed insertion in the latter two strains of a TTTA repeat that created a frameshift and resulting premature stop codon at amino acid 203 (Fig. 1A). This truncation eliminated the region encoding the choline binding domain and, as predicted, resulted in an inability to retain the N

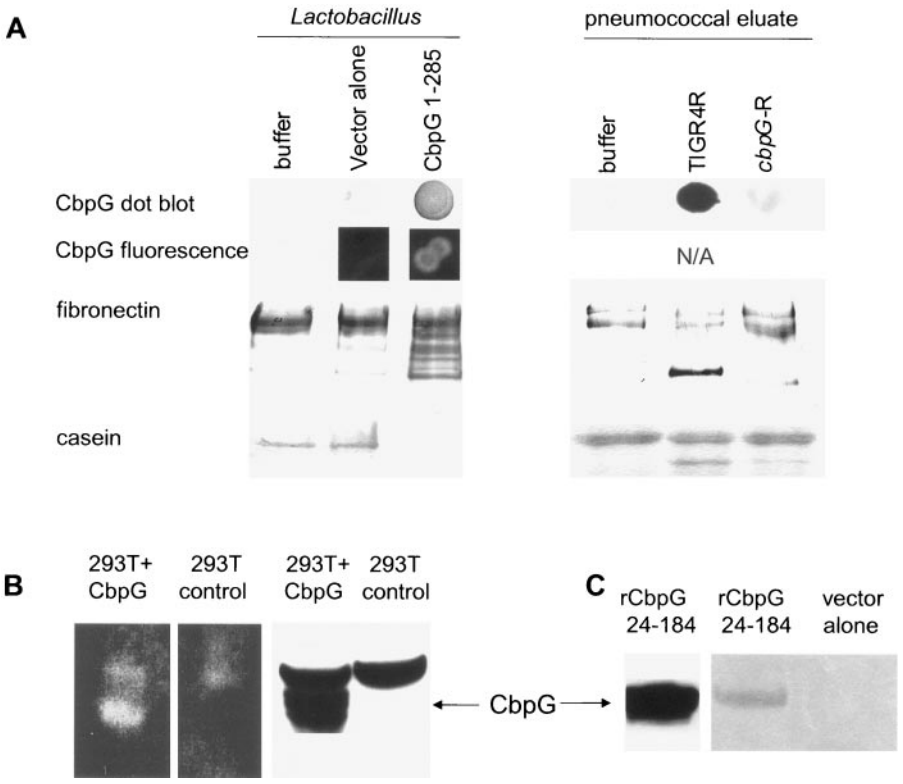

FIG. 2. Proteolysis of fibronectin and α-casein. (A) Expression of CbpG amino acids 1 to 285 (CbpG 1–215) on intact *L. casei* cells (left panel) or in pneumococcal choline eluates of different strains (right panel) was measured by dot blotting with anti-CbpG antibody. For lactobacilli, surface expression of CbpG was also confirmed by whole-cell fluorescence of intact bacteria probed with anti-CbpG antibody (N/A, not applicable to eluate). Proteolysis of fibronectin and α-casein was analyzed by Western blotting or by SDS-PAGE. (B) Proteolytic activity of rCbpG expressed in 293T cells as assessed with a zymogram against casein (293T cells show an endogenous proteolytic band independent of rCbpG). A Western blot of 293T cell lysates is shown on the right. (C) Proteolytic activity of truncated rCbpG expressed in *E. coli* as assessed by production of a cleavage product of casein, shown by Coomassie blue staining of an SDS-PAGE gel.

terminus on the bacterial surface (Fig. 1E). To determine the prevalence of this *cbpG* mutation, clinical isolates from diverse sites of pneumococcal disease were obtained. For each isolate, the *cbpG* gene was amplified by PCR from genomic DNA and sequenced. The sequence results showed that 27% (6 of 22) of healthy pneumococcal carriers, 35% (7 of 20) of pneumonia isolates, 25% (6 of 24) of meningitis strains, and 5% (1 of 19) of otitis media isolates exhibited the truncated form of *cbpG*. In every instance, truncation was due to the same insertion of the TTTA tetramer. Thus, both full-length and truncated forms of CbpG have clinical relevance. The mutant studied previously (11) expressed a truncated protein encompassing the protease domain (amino acids 1 to 215) (Fig. 1A). To compare not only truncated but also null mutants to the wild type, newer technology was used to create a complete *cbpG* deletion.

The TIGR4 genome database indicated that *cbpG* was flanked upstream by two hypothetical proteins (SP0388 and SP0389) and a two-component system (SP0386 and SP0387) and was followed 22 bp downstream by *cbpF* (SP0391) (11) (Fig. 1B). Northern blot analysis was used to determine expression of *cbpG* during the growth cycle. Bacterial lysates from the lag, midlog, stationary, and late stationary phases were probed with ^{32}P-labeled *cbpG* DNA, and the results revealed that there was *cbpG* expression throughout the growth cycle, although the level was lower in the late stationary phase (data not shown). Three transcripts were identified with the *cbpG* probe in wild-type RNA (Fig. 1B and C). A probe for the histidine kinase gene identified the largest of the three transcripts, consistent with cotranscription of the two-component system, the hypothetical proteins, *cbpG*, and *cbpF*. Microarray analysis indicated that the absence of the histidine kinase resulted in 2.5- to 4.4- ± 0.06-fold upregulation of all four tandem genes downstream of the two-component system (both hypothetical genes, *cbpG*, and *cbpF*). While this suggests that there is coordinate regulation, it is still possible that upregulation could be the result of readthrough beyond the inserted erythromycin resistance cassette. Northern analysis of *cbpG*- RNA revealed a band consistent with a transcript reading through the *erm* replacement cassette into *cbpF* (Fig. 1C). A *cbpF* probe for this blot revealed the same pattern in the wild type as in the *cbpG*- mutant, and Western analysis confirmed that there was expression of CbpF (Fig. 1D), indicating that at least under these conditions, the mutation of *cbpG* did not cause polar effects on transcription.

CbpG protease activity. The potential protease activity of CbpG was assayed in several settings. *L. casei* cells expressing rCbpG attached to the cell wall via LPXTG were incubated with fibronectin or casein. Dot blot and whole-cell fluorescence analyses indicated that *L. casei* with pLPMSSA4/cbpG1-285 ex-

A

Adherence of CbpG- mutants (% of wild type)

	Detroit	A549	$RBCEC_6$
cbpG-$_{KKG}$R	11±3	12±4	25±5
cbpG-R	13±3	20±4	27±5

B

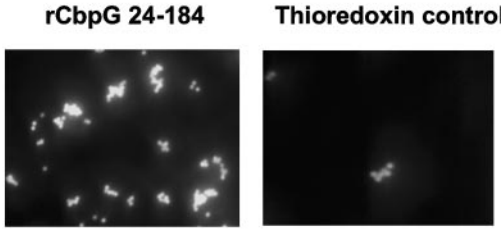

FIG. 3. Role of CbpG in adherence. (A) Adherence assay performed with cell lines for the isogenic truncated *cbpG-*$_{KKG}$R mutant or the complete deletion mutant *cbpG-R*. The results are expressed as percentages of the value for wild-type TIGR4R, for which 112 ± 14 bacteria/well was defined as 100%. The values are means ± standard deviations of three independent experiments. (B) Adherence of rCbpG-coated beads to $RBCEC_6$ endothelial cells.

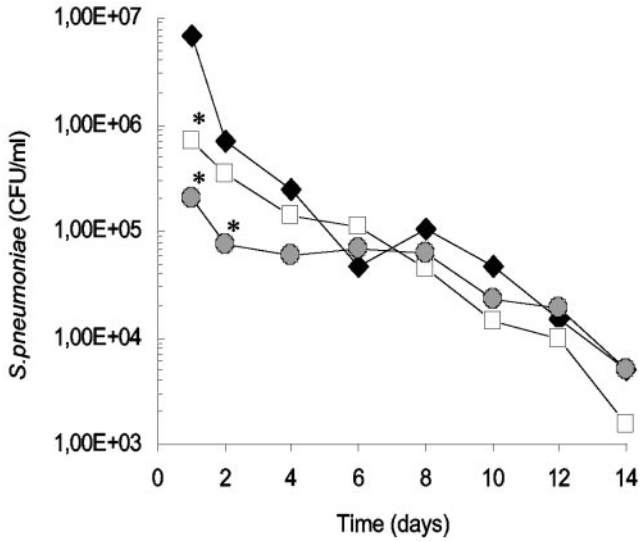

FIG. 4. Effect of CbpG on colonization. *S. pneumoniae* parent strain TIGR4 (diamonds) was compared to encapsulated *cbpG-*$_{KKG}$ (circles) and *cbpG-* (squares) in a nasopharyngeal colonization model. Mice were challenged intranasally with 10^7 CFU, and bacterial titers were determined by nasopharyngeal lavage. The symbols indicate the median titer for each group (6 to 10 mice) at each time postinfection. Asterisks indicate that there were statistically significant differences ($P < 0.05$) in the bacterial titers when the mutant strains and the wild type were compared using a Mann-Whitney nonparametric analysis.

pressed extracellular, surface-associated CbpG and degraded both fibronectin and α-casein (Fig. 2A, left panel). This activity was inhibited by anti-CbpG antibody (data not shown). In contrast, *L. casei* with the empty vector pLPMSSA4 was negative in all assays. Eluates of TIGR4R degraded fibronectin and α-casein more effectively than the null mutant strain TIGR4R *cbpG-* (Fig. 2A, right panel). rCbpG expressed in eukaryotic cells (Fig. 2B) or truncated CbpG expressed in *E. coli* (Fig. 2C) hydrolyzed casein. The relative specific activity of cell-bound versus released CbpG was not determined; it is possible that there were changes in activity with a loss of surface anchoring.

Role of CbpG in adherence in vitro. To determine the relationship of the proteolytic activity of CbpG to its previously described adhesive activity, the two CbpG- mutants were assessed for adherence to Detroit nasopharyngeal epithelia, A549 lung epithelia, and $RBCEC_6$ brain endothelia. Elimination of the entire gene or truncation of the cell wall anchor decreased adherence >70%, and there was no difference between the mutants. This was documented for all three cell types (Fig. 3A). Thus, the function of CbpG in adherence required the choline binding domain surface anchor. To further document the adhesive activity of CbpG, beads were coated with rCbpG, and attachment to endothelial cells was tested (Fig. 3B). Beads coated with rCbpG24-184 adhered at a mean level of 148 ± 22 beads/field, in contrast to the control beads bearing thioredoxin, which adhered at a level of 43 ± 27 beads/field.

Role of CbpG in colonization and invasive disease. CbpG could contribute to virulence by virtue of proteolytic activity or adhesive activity or both. *S. pneumoniae* was quantified from nasal lavages of mice challenged intranasally with 10^7 CFU of TIGR4, *cbpG-*$_{KKG}$, and *cbpG-* (Fig. 4). Consistent with the colonization defect determined previously, the titers for mice infected with *cbpG-*$_{KKG}$ and *cbpG-* on day 1 were 10- to 80-fold lower than those for mice infected with TIGR4. No differences were observed between the two mutants, and all strains were similar after 2 days. This suggested that proteolytic bioactivity of the truncated CbpG did not play a role in colonization. However, the possibility that proteolytic activity of CbpG may be decreased without a cell wall anchor if its target must be close to the bacterial surface cannot be ruled out.

To determine the role of CbpG in pneumonia, mice were challenged intratracheally with 10^6 CFU of bioluminescent TIGR4X, *cbpG-*$_{KKG}$X, or *cbpG*-X and imaged at 24 h postinfection. Bacterial titers from in vivo samples were used to corroborate images obtained with the Xenogen imaging system (Fig. 5A). Only mice infected with wild-type strain TIGR4X developed pneumonia (Fig. 5B). Quantitation of the bacterial titers confirmed that there was severe pneumonia in mice infected with TIGR4X (10^7 to 10^8 CFU/mg of lung tissue) and that there were 2-log-fewer bacteria in mice infected with *cbpG-*$_{KKG}$X and *cbpG*-X (10^5 to 10^6 CFU/mg of lung tissue) ($P = 0.003$). These results are consistent with the decreased adherence of both CbpG- bacteria to lung epithelial cells in vitro.

In order to determine the role of CbpG in invasive disease, bacterial titers were determined in blood of mice that were infected intratracheally (Fig. 5A) and in a second set of mice that were infected intravenously (Fig. 5C). Mice that were infected intratracheally with TIGR4X developed significantly higher bacterial titers in the blood (10^6 to 10^7 CFU/ml) than mice that were infected with *cbpG-*$_{KKG}$X and *cbpG*-X developed (10^6 and 10^4 CFU/ml of blood) ($P = 0.04$). The most striking difference in virulence was seen in mice challenged intravenously with the three strains. Bioluminescent imaging of mice

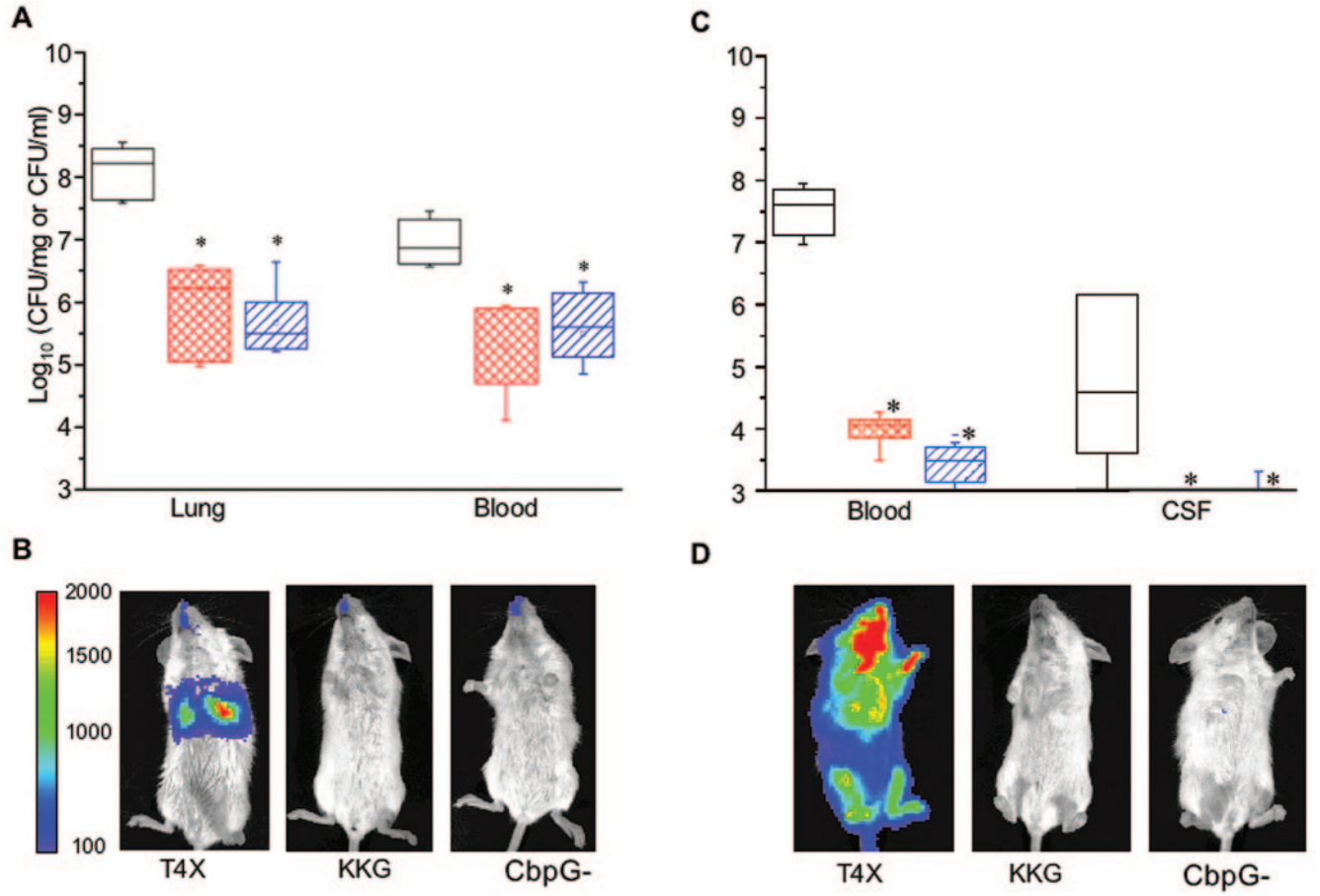

FIG. 5. Effect of CbpG on pneumonia. (A) Bacterial titers in the lungs and blood of mice challenged intratracheally with 10^6 CFU of TIGR4X (open boxes) or encapsulated mutant *cbpG*-$_{KKG}$X (blue boxes) or *cbpG*-X (red boxes) (6 to 10 mice per group). The boxes indicate the ranges; the lines indicates the means; and the error bars indicate the standard deviations. Asterisks indicate that there were statistically significant differences ($P < 0.05$) in the bacterial titers when means of the mutant strains and the wild type were compared by a Mann-Whitney nonparametric analysis. (B) Representative bioluminescent images of mice from the experiment whose results are shown in panel A obtained using the IVIS charge-coupled device camera (Xenogen Corporation). Bacterial density correlates with photon intensity. (C) Bacterial titers in the blood and CSF of mice challenged intravenously with 10^5 CFU of TIGR4X (open boxes) or encapsulated mutant *cbpG*-$_{KKG}$X (blue box) or *cbpG*-X (red box) (6 to 10 mice per group). (D) Bioluminescent images of representative mice from the experiment whose results are shown in panel C. T4X, strain TIGR4X; KKG, strain *cbpG*-$_{KKG}$X; CbpG-, strain *cbpG*-X.

challenged with 10^5 CFU of TIGR4X and the *cbpG*- mutants intravenously confirmed that both mutants were dramatically attenuated in the ability to survive or replicate in the bloodstream or in the ability to enter the CSF, in contrast to the wild type (Fig. 5C and D). The bacterial titers corroborated these images; 10^7 pneumococci/ml was isolated from the blood of animals infected with TIGR4X, whereas only 10^3 to 10^4 CFU/ml was obtained from the blood of mice infected with *cbpG*-$_{KKG}$X or *cbpG*-X. The bacterial titers obtained from CSF were also different. The TIGR4X titers ranged from 10^3 to 10^6 CFU/ml, whereas no bacteria were detected in the CSF of mice challenged with the mutants ($P = 0.006$).

To determine the ability of CbpG to act as a protective antigen, mice were vaccinated and challenged with wild-type bacteria, and colonization and bacteremia were monitored. All CbpG-vaccinated mice developed serum antibody to CbpG. At 24 and 48 h after challenge, vaccinated mice remained active, while the control group was visibly sick. Vaccination with CbpG provided a low but statistically significant degree of protection against colonization and substantial protection against systemic infection. At 72 h, control mice were colonized in the nasopharynx at a level of 3.8×10^7 to 5.1×10^7 CFU/ml, while vaccinated mice harbored 1.4×10^7 to 1.8×10^7 CFU/ml ($P < 0.05$). The median blood titer of CbpG-vaccinated mice was 10^4 CFU/ml at 48 h and remained at or below this level until day 7, and 50% of the mice survived for 7 days. In contrast, in control mice there was a steady increase in the blood titers to 10^7 CFU/ml, and 83% of the mice died by 7 days ($P < 0.03$).

DISCUSSION

CbpG is notable among the Cbps in that it plays a role in virulence in models of both mucosal colonization and sepsis (11). A segment of the N terminus of CbpG exhibited 47% sequence homology to trypsin-like serine proteases. Degradation of fibronectin and α-casein by lactobacilli expressing surface-bound CbpG and CbpG eluted from pneumococci, as well

as by either full-length or truncated rCbpG, indicated that CbpG has proteolytic activity. CbpG is probably not the only pneumococcal protease that can hydrolyze fibronectin, and its possible substrate preference over other pneumococcal proteases remains to be determined (5, 13, 31).

Sequence analysis of *cbpG* from a variety of laboratory and clinical isolates showed that this gene had two alleles. One-third of the isolates from the nasopharynges of healthy carriers and blood isolates from both pneumonia and meningitis patients carried a CbpG truncation resulting from introduction of a stop codon prior to the choline binding domain, which eliminated the mechanism of attachment of the protein to the bacterial surface. Proteolytic activity was detected whether the enzyme was bound to a bacterial surface by choline or not. This contrasts with another Cbp, LytA, which must adsorb to the cell wall substrate via choline in order to be active, and its activity is enhanced by dimerization in the presence of the choline binding domain (6, 10). Since both full-length and truncated CbpG variants were found in isolates obtained from invasive disease, truncation of CbpG does not appear to eliminate disease potential. This argues for in vivo significance for proteolysis by CbpG since adherence activities are lost in the secreted variant. However, in the animal models tested, we were unable to identify a phenotype that was retained by the truncated mutant but lost by the complete CbpG null mutant that would indicate the role of proteolysis in pathogenesis.

rCbpG was shown to support binding of beads to eukaryotic cells. In contrast to proteolysis, the adherence capacity of CbpG required the presence of the choline binding domain, a finding consistent with the need to bridge bacterial and host cell surfaces during adhesion. CbpG is the first example of allelic variability in the presence of the surface-anchoring choline binding domain. This could allow modulation of adherence without sacrificing proteolysis but does not rule out the possibility that proteolysis may be required for adherence. Mapping of the proteolytic domain and creation of a nonproteolytic mutation are required to distinguish these possibilities.

Secreted or surface-associated proteases of bacterial pathogens often have more than one activity in host cell interactions. The first example of such a multifunctional protease was the hemagglutinin/protease of *Vibrio cholerae* (7). Other identified surface proteases, adhesins, or invasins include the C5a peptidase of group B streptococci (2, 4, 15) and immunoglobulin A1 protease of gonococci (14). The most prominent example of a multifunctional surface protease is Pla of *Y. pestis.* Pla activates plasminogen into plasmin that degrades the extracellular matrix and cleaves complement C3, reducing phagocytosis. Pla also proteolytically cleaves α_2-antiplasmin, the major inhibitor of plasmin, and possibly promotes uncontrolled proteolysis (18). CbpG may also be a multifunctional protease. We demonstrated that CbpG is necessary for pneumococcal virulence at multiple anatomical sites and can be used as an effective vaccine to decrease colonization and invasive disease. As a matrix protease, it is active when it is anchored on the bacterial surface and in the secreted form. In contrast, CbpG must be attached to the bacterium to be a functional adhesin. Modification of function depending on release or attachment to the bacterial surface is a novel virulence attribute that may apply to other choline binding protein family members.

REFERENCES

1. **Antikainen, J., L. Anton, J. Sillanpää, and T. K. Korhonen.** 2002. Domains in the S-layer protein CbsA of *Lactobacillus crispatus* involved in adherence to collagens, laminin and lipoteichoic acids and in self-assembly. Mol. Microbiol. **46:**381–394.
2. **Beckmann, C., J. Waggoner, T. Harris, G. Tamura, and C. Rubens.** 2002. Identification of novel adhesins from group B streptococci by use of phage display reveals that C5a peptidase mediates fibronectin binding. Infect. Immun. **70:**2868–2876.
3. **Blasig, I., H. Giese, M. Schroeter, A. Sporbert, D. Utepbergenov, I. Buchwalow, K. Neubert, G. Schonfelder, D. Freyer, I. Schiimke, W. Siems, M. Paul, R. Haseloff, and R. Blasig.** 2001. ∗NO and oxyradical metabolism in new cell lines of rat brain capillary endothelial cells forming the blood brain barrier. Microvasc. Res. **62:**114–127.
4. **Cheng, Q., D. Stafslien, S. Purushothaman, and P. Cleary.** 2002. The group B streptococcal C5a peptidase is both a specific protease and an invasin. Infect. Immun. **70:**2408–24113.
5. **Courtney, H.** 1991. Degradation of connective tissue proteins by serine proteases from *Streptococcus pneumoniae*. Biochem. Biophys. Res. Commun. **175:**1023–1028.
6. **Fernandez-Tornero, C., R. Lopez, E. Garcia, G. Gimenez-Gallego, and A. Romero.** 2001. A novel solenoid fold in the cell wall anchoring domain of the pneumococcal virulence factor LytA. Nat. Struct. Biol. **8:**1020–1024.
7. **Finkelstein, R., and L. Hanne.** 1982. Purification and characterization of the soluble hemagglutinin (cholera lectin) produced by *Vibrio cholerae*. Infect. Immun. **36:**1199–1208.
8. **Francis, K., J. Yu, C. Bellinger-kawahara, D. Joh, J. Hawkinson, M. Xiao, T. Purchio, M. Caparon, M. Lipsitch, and P. Contag.** 2001. Visualizing pneumococcal infection in the lungs of live mice using bioluminescent *Streptococcus pneumoniae* transformed with a novel gram-positive lux transposon. Infect. Immun. **69:**3350–3358.
9. **Garcia, J., R. Sanchez-Beato, F. Medrano, and R. Lopez.** 1998. Versatility of choline-binding domain. Microb. Drug Res. **4:**25–36.
10. **Garcia-Bustos, J., and A. Tomasz.** 1987. Teichoic acid containing muropeptides from *Streptococcus pneumoniae* as substrates for the pneumococcal autolysin. J. Bacteriol. **169:**447–453.
11. **Gosink, K., E. Mann, C. Guglielmo, E. Tuomanen, and R. Masure.** 2000. Role of novel choline binding proteins in virulence of *Streptococcus pneumoniae*. Infect. Immun. **68:**5690–5695.
12. **Haas, W., D. Kaushal, J. Sublett, C. Obert, and E. Tuomanen.** 2005. Vancomycin stress response in a sensitive and a tolerant strain of *Streptococcus pneumoniae*. J. Bacteriol. **187:**8205–8210.
13. **Holmes, A., R. McNab, K. Millsap, M. Rohde, S. Hammerschmidt, J. Mawdsley, and H. Jenkinson.** 2001. The *pavA* gene of *Streptococcus pneumoniae* encodes a fibronectin-binding protein that is essential for virulence. Mol. Microbiol. **41:**1395–1408.
14. **Hopper, S., B. Vasquez, A. Merz, S. Clary, J. Wilbur, and M. So.** 2000. Effects of the immunoglobulin A1 protease on *Neisseria gonorrhoeae* trafficking across polarized T84 epithelial monolayers. Infect. Immun. **68:**906–911.
15. **Hytönen, J., S. Haataja, D. Gerlach, A. Podbielski, and J. Finne.** 2001. The SpeB virulence factor of *Streptococcus pyogenes*, a multifunctional secreted and cell surface molecule with strepadhesin, laminin-binding and cystein protease activity. Mol. Microbiol. **39:**512–519.
16. **Kukkonen, M., and T. K. Korhonen.** 2004. The omptin family of enterobacterial surface proteases/adhesins: from housekeeping in *Escherichia coli* to systemic spread of *Yersinia pestis*. Int. J. Med. Microbiol. **294:**7–14.
17. **Lacks, S., and R. Hotchkiss.** 1960. A study of the genetic material determining an enzyme activity in pneumococcus. Biochim. Biophys. Acta **39:**508–517.
18. **Lähteenmäki, K., M. Kukkonen, and T. K. Korhonen.** 2001. The Pla surface protease/adhesin of *Yersinia pestis* mediates bacterial invasion into human endothelial cells. FEBS Lett. **504:**69–72.
19. **Martinez, B., J. Sillanpää, E. Smit, T. K. Korhonen, and P. Pouwels.** 2002. Expression of *cbsA* encoding the collagen-binding S-protein of *Lactobacillus crispatus* JCM5810 in *Lactobacillus casei* ATCC 393^T. J. Bacteriol. **182:**6857–6861.
20. **McDaniel, L. S., J. S. Sheffield, P. Delucchi, and D. E. Briles.** 1991. PspA, a surface protein of *Streptococcus pneumoniae*, is capable of eliciting protection against pneumococci of more than one capsular type. Infect. Immun. **59:**222–228.
21. **Orihuela, C., G. Gao, M. McGee, J. Yu, K. Francis, and E. Tuomanen.** 2003. Organ specific models of *Streptococcus pneumoniae* disease. Scand. J. Infect. Dis. **35:**647–652.
22. **Pouttu, R., B. Westerlund-Wikström, H. Lång, K. Alsti, R. Virkola, U. Saarela, A. Siitonen, N. Kalkkinen, and T. K. Korhonen.** 2001. *matB*, a common fimbrillin gene of *Escherichia coli*, expressed in a genetically conserved, virulent clonal group. J. Bacteriol. **183:**4727–4736.
23. **Pouwels, P., A. Vriesema, B. Martinez, F. Teielen, J. Seegers, J. Leer, J. Jore, and E. Smit.** 2001. Lactobacilli as vehicles for targeting antigens to mucosal

tissues by surface exposition of foreign antigens. Methods Enzymol. **336:**369–389.
24. **Ronda, C., J. Garcia, E. Garcia, J. Sanchez-Puelles, and R. Lopez.** 1987. Biological role of the pneumococcal amidase: cloning of the *lytA* gene in *Streptococcus pneumoniae*. Eur. J. Biochem. **164:**621–624.
25. **Rosenow, C., P. Ryan, J. Weiser, S. Johnson, P. Fontan, A. Ortqvist, and H. Masure.** 1997. Contribution of a novel choline binding protein to adherence, colonization, and immunogenicity of *Streptococcus pneumoniae*. Mol. Microbiol. **25:**819–829.
26. **Sanchez-Puellas, J., J. Garcia, R. Lopez, and E. Garcia.** 1987. 3′-End modifications of the *Streptococcus pneumoniae lytA* gene: role of the carboxy terminus of the pneumococcal autolysin in the process of enzymatic activation. Gene **61:**13–19.
27. **Talkington, D. F., D. L. Crimmins, D. C. Voellinger, J. Yother, and D. E. Briles.** 1991. A 43-kilodalton pneumococcal surface protein, PspA: isolation, protective abilities, and structural analysis of the amino-terminal sequence. Infect. Immun. **59:**1285–1289.
28. **Tettelin, H., K. E. Nelson, I. T. Paulsen, J. A. Eisen, T. D. Read, S. Peterson, J. Heidelberg, R. T. DeBoy, D. H. Haft, R. J. Dodson, A. S. Durkin, M. Gwinn, J. F. Kolonay, W. C. Nelson, J. D. Peterson, L. A. Umayam, O. White, S. L. Salzberg, M. R. Lewis, D. Radune, E. Holtzapple, H. Khouri, A. M. Wolf, T. R. Utterback, C. L. Hansen, L. A. McDonald, T. V. Feldblyum, S. Angiuoli, T. Dickinson, E. K. Hickey, I. E. Holt, B. J. Loftus, F. Yang, H. O. Smith, J. C. Venter, B. A. Dougherty, D. A. Morrison, S. K. Hollingshead, and C. M. Fraser.** 2001. Complete genome sequence of virulent isolates of *Streptococcus pneumoniae*. Science **293:**498–506.
29. **Tomasz, A., A. Albino, and E. Zanati.** 1970. Multiple antibiotic resistance in a bacterium with suppressed autolytic system. Nature **227:**138–140.
30. **Tu, A., R. Fulgham, M. McCrory, D. Briles, and A. Szalai.** 1999. Pneumococcal surface protein A inhibits complement activation by *Streptococcus pneumoniae*. Infect. Immun. **67:**4720–4724.
31. **van der Flier, M., N. Chhun, T. Wizemann, J. Min, J. McCarthy, and E. Tuomanen.** 1995. Adherence of *Streptococcus pneumoniae* to immobilized fibronectin. Infect. Immun. **63:**4317–4322.
32. **Weiser, J., R. Austrian, P. Sreenivasan, and H. Masure.** 1994. Phase variation in pneumococcal opacity: relationship between colonial morphology and nasopharyngeal colonization. Infect. Immun. **62:**2582–2589.

Editor: J. N. Weiser